

Climate characteristics and factors behind heavy rainfall during the Baiu¹ season in 2023 and extremely high temperatures from mid-July onward

28 September 2023

Tokyo Climate Center (TCC), Japan Meteorological Agency (JMA)

<https://www.data.jma.go.jp/tcc/tcc>

Summary

The climate characteristics and factors behind heavy rainfall during the Baiu season in 2023 and extremely high temperatures in summer 2023 can be summarized as follows:

- Heavy rainfall from June to mid-July 2023
 - The Baiu front stagnated near Japan's main island of Honshu in early June, and a series of stationary linear mesoscale convective systems (SLMCSs) hit the Pacific side of eastern and western Japan (Figure A1). Such conditions brought unprecedented 24-hour June rainfall at 167 stations. Enhanced frontal activity over brought heavy rain over a wide area from western to northern parts of the country from late June to mid-July, accompanying SLMCSs in western Japan and elsewhere.
 - The widespread heavy rain observed during the Baiu season is associated with large amounts of warm moist air flowing over Japan and increased frontal activity. The inflow of large amounts of water vapor was associated with Typhoon Mawar, which moved eastward over the sea to the south of Japan in early June, and with a strengthened Pacific High to the south of Japan from late June onward. The heavy rainfall observed may also have been associated with an increasing volume of water vapor caused by long-term global warming.
- Extremely high temperatures from mid-July 2023 onward
 - Record-high temperatures were observed in northern/eastern Japan and elsewhere from mid-July onward. The average temperature for northern Japan in late July was the highest for the region since records began in 1946, and that for eastern Japan was the second highest for the region. The average temperature for the Sea of Japan side of eastern and western Japan in early August was also the highest ever. From July 16 to August 23, 106 of 915 observation stations in Japan saw record-high maximum temperatures. The national average surface temperature over summer was the highest since records began in 1898.

¹ The Baiu is a period of cloudy and rainy weather in early summer in Japan. The phenomenon is climatologically characterized by the stagnation of a Baiu front extending from west to east.

- The significantly high temperatures observed in the second half of July are attributed to active cumulus convection and typhoons near the Philippines, which caused the upper-level subtropical jet stream (STJ) to shift northward and a warm anticyclone to cover Japan, and the extension of the low-level Pacific High toward Japan strengthened to a record level. The conditions near the Philippines may have been due to weaker-than-normal cumulus convective activity over the tropical Indian Ocean due to the La Niña event that ended in winter 2022/2023. The northward shift of the STJ near Japan may also have been associated with the meandering of the jet stream over Europe and the Mediterranean. In addition to the pronounced northward shift of the STJ, Typhoons Khanun and Lan continued bringing warm, moist air from the south to Japan in the first half of August, and the influence of Foehn phenomena added to the record high temperatures on the Sea of Japan side. The remarkably high temperatures observed during summer are attributed to a worldwide summer tendency associated with persistent global warming. The record-high temperatures in northern Japan may also have been influenced by significantly higher temperatures in surrounding seas.

Introduction

This report summarizes discussions held by the TCC Advisory Panel on Extreme Climatic Events (a Japan Meteorological Agency (JMA) body staffed by prominent climate science academics and researchers) on 28 August 2023 to identify possible causative factors for the extreme meteorological conditions observed. Accordingly, the content applies as of 28 August 2023 (except for certain statistics).

Analysis of large-scale atmospheric circulation is based on field data from JMA's Third Long-Term Reanalysis (JRA-3Q)².

1. Climate characteristics and factors behind heavy rainfall from June to mid-July

(1) Heavy rainfall

The Baiu front remained stagnant near Honshu (Japan's main island) in early June. Warm, moist air flow associated with Typhoon Mawar (which moved eastward from the vicinity of Okinawa to the sea south of eastern/western Japan) increased the activity of the front, resulting in heavy rainfall. In particular, a series of stationary linear mesoscale convective systems (SLMCSs) formed over the Pacific side of eastern and western Japan. Unprecedented 24-hour precipitation for June was recorded at 167 observation stations, with 23 also recording historical highs for the whole year (Figure 1-1).

On June 28, warm, moist air began flowing toward the Baiu front, which stagnated near Japan resulting in heavy rainfall, including SLMCSs in many places. Total precipitation from June 28 to July 16 exceeded 1,200 mm at several stations in northern Kyushu region (Figure 1-2), and double the normal monthly rainfall for July was seen at some stations in the Hokkaido, Tohoku, San'in and northern Kyushu regions (including Yamaguchi Prefecture) (Figure 1-3).

From June 28 to July 6, heavy rain fell nationwide except for the Okinawa region and northern Japan, partly due to upper cold air. From July 1 to 3, SLMCSs formed in the prefectures of Yamaguchi and Kumamoto and Amami region.

From July 7 to 10, heavy rain fell in the northern Kyushu and Chugoku regions and elsewhere (Figure 1-4). SLMCSs formed in Shimane Prefecture on July 8 and in northern Kyushu on July 10. In response, JMA issued heavy-rain emergency warnings for the prefectures of Fukuoka and Oita on the morning of July 10. From July 11 to 13, in addition to the Baiu front near Honshu, a low-pressure system passed Hokkaido, causing heavy rain over a wide area from western to northern Japan. On July 12, SLMCSs formed in the prefectures of Ishikawa and Toyama. From July 14 to 16, total rainfall exceeded 400 mm in some places, with unprecedented levels in Akita Prefecture and elsewhere (Figure 1-5).

(2) Characteristics of large-scale atmospheric circulation associated with heavy rainfall

² https://jra.kishou.go.jp/JRA-3Q/index_en.html

(a) Early June

- From June 1 to 3, the Baiu front near Honshu became more active, mostly due to the effects of large amounts of water vapor flowing in with Typhoon Mawar to the south Japan.
 - The amount of northward water vapor transport (Figure 1-6) over the sea south of Honshu was largest on record for early June and comparable to the record for the second half of the Baiu season.

(b) Late June to mid-July

The characteristics of average atmospheric circulation from late June to mid-July are described below, with numbers in parentheses corresponding to Figure 1-7.

- The Pacific High extended strongly westward to the south of Japan (1), and intensified air flows along its edge facilitated the transportation of large amounts of water vapor to the vicinity of the country (2). Baiu front activity near Japan also increased. In addition, the upper-level STJ strengthened from China to Japan and meandered southward to the west of Japan (3), which likely contributed to sustained upward motion near the Baiu front to the south of the STJ.
 - The strength of the Pacific High to the south of Japan may be related to increased cumulus convective activity near Indonesia. The weak extension of the Pacific High near Japan may have been due to the ongoing El Niño conditions.
- From July 7 to 10, when record-breaking heavy rain fell in the northern Kyushu region and elsewhere, a large amount of water vapor flowed to the region from around central China, and an upper-level trough forming to the west of Japan caused STJ meandering. The Baiu front also became particularly active (Figure 1-8).
- From July 14 to 16, when record-breaking heavy rain fell in Akita Prefecture in northern Japan and elsewhere, a tropical cyclone near the Philippines was about to develop into Typhoon Talim, and the Pacific High was extending toward Japan. As a result, a large amount of water vapor from the tropics flowed over the Sea of Japan along the edge of the High, and the Baiu front, which had stalled near the Tohoku region, became particularly active (Figure 1-9).

(c) SLMCS over northern Kyushu

In the northern Kyushu region (to the south of the Baiu front, which stalls from central China to the Korea Strait), there was a noticeable low-level inflow of warm, humid air around the edge of the Pacific High, and an SLMCS formed on the morning of July 10. Unprecedentedly heavy rain was observed, with emergency warnings issued for the prefectures of Fukuoka and Oita. Rain falling at a rate of 91.5 mm/h was observed in Minousan in Fukuoka Prefecture. The SLMCS was composed of multiple cumulonimbus clouds extending from the southwest to the northeast, and its formation process appears to have been a backbuilding type.

Regarding environmental field characteristics, there was a large amount of water vapor

low-level inflow from the southwest around the edge of the Pacific High near northern Kyushu (Figure 1-10, left). The air mass flowing in from the sea to the west of Kyushu was warm and humid at approximately 500 m (Figure 1-10, right). Thick, humid air masses also flowed in from the west along the Baiu front. Heavy rain on the morning of July 10 accompanied atmospheric conditions favorable for enhanced convection due to a temperature decrease of around 2 degrees at 500 hPa (an altitude of approx. 5,880 m) from the previous day and the influence of upward flow associated with a trough in the mid-level troposphere that moved eastward to the north of Kyushu.

(3) Effects of global warming on precipitation

The long-term frequency of extreme heavy rainfall in Japan shows an increasing tendency. For example, the annual number of heavy-rain events producing 100 mm or more over 3 hours at AMeDAS stations in the last 10 years has increased by a factor of approximately 1.6 as compared to around 1980 (Figure 1-11). One factor behind this is a long-term increase in atmospheric water vapor content associated with global warming (Figure 1-12).

Under the MEXT (Ministry of Education, Culture, Sports, Science and Technology, Japan)-Program for the Advanced Studies of Climate Change Projection (SENTAN) , preliminary Event Attribution³ experiments in relation to the heavy rain observed in the northern Kyushu region from July 9 to 10 were performed to assess the effects of global warming using a high-resolution model. The results showed that the amount of precipitation over land in northern Kyushu was higher in the current-climate experiment than in the non-warming experiment, which assumed no rise in temperature due to global warming (Figure 1-13). The outcomes suggest that this rain event may have been particularly heavy due to global warming.

2. Climate characteristics and factors behind extremely high temperatures from mid-July 2023 onward

(1) High temperatures

In the second half of July, the Pacific High extended to Honshu, resulting in record-high temperatures in northern Japan and elsewhere (Figure 2-1). The average temperature anomaly in late July was +3.9°C in northern Japan, which was the highest since records began in 1946. The figure for eastern Japan was +1.9°C, which was the second highest on record.

In early August the Pacific High retreated to the east of Japan, but warm, humid air continued to flow in along the edge of the high-pressure with the slow-moving typhoons Khanun and Lan. As a result, temperatures remained significantly higher than normal in northern Japan and on the Sea of Japan side of eastern and western Japan. Due to the influence of Foehn phenomena caused by the inflow of moist air from the south, a temperature of 40.0°C was

³ A method for probabilistic estimation of how much the occurrence of individual phenomena has changed due to global warming by comparing a number of simulation experiments conducted under past climate conditions using a climate model and simulations conducted under a scenario with no global warming caused by human activity.

observed in Komatsu in Ishikawa Prefecture on August 10. Temperatures did not drop at night, and the daily-minimum temperature in Itoigawa in Niigata Prefecture on August 10 was 31.4°C, breaking the all-time record for highest daily-minimum temperature in Japan. These two prefectures are located on the Sea of Japan side, namely the leeward side of mountain ranges. The average temperature anomaly in early August was significantly high in northern, eastern and western Japan, with the Sea of Japan sides of eastern and western Japan at +3.4°C and +2.1°C, respectively – the highest since records began in 1946.

Late July to early August is the hottest period of the year even in normal years, and a temperature of 40°C was observed in Yanagawa in Fukushima Prefecture on August 5. From July 16 to August 23, 106 of 915 observation stations across the country recorded unprecedented highest daily-maximum temperatures for the entire year. In Tokyo there were 13 extremely hot days (maximum temperatures higher than 35°C) in July, significantly exceeding the 7 days of 2001 and the highest number of days ever observed in July. Figure 2-2 summarizes the number of extremely hot days observed in AMeDAS data nationwide from June 1 to August 31. For comparison, past years with particularly hot summers were 2010, 2013, 2018 and 2022. In 2023, the number of stations recording extremely hot days increased significantly from the latter half of July onward, reaching almost the same level as 2018 by mid-August.

In July 2023, Japan's average surface temperature,⁴ which is used to monitor long-term changes such as global warming, reached +1.91°C above the base value (the 30-year average for 1991 – 2020). This was the highest since records began in 1898, surpassing the previous high of +1.51°C in 1978 (Figure 2-3). The national average temperature anomaly for summer (June – August) was +1.76°C, also the hottest for summer on record, surpassing the previous value of +1.08°C in 2010. June was the second-hottest month on record, and August was the hottest.

(2) Characteristics of large-scale atmospheric flow bringing remarkably high temperatures

(a) Second half of July onward

The climate characteristics and factors behind the large-scale atmospheric circulation bringing remarkably high temperatures in the second half of July are outlined below, with numbers in parentheses corresponding to Figure 2-4.

- In the vicinity of Japan, the extension of Pacific High ((1)) in the lower level became noticeably stronger, especially in the second half of July (Figure 2-5), and persistent descent motions and strong solar radiation from clear skies caused surface temperatures to rise. The upper-level STJ near Japan clearly shifted northward ((2)), and the country

⁴ The calculation of Japan's average temperature anomalies to the normal is based on observations at 15 stations (Abashiri, Nemuro, Sutsu, Yamagata, Ishinomaki, Fushiki, Iida, Choshi, Sakai, Hamada, Hikone, Miyazaki, Tadotsu, Nase and Ishigakijima) selected to ensure long-term homogeneity of observation data and a relatively small environmental change due to urbanization, etc., and distributed regionally without bias.

was covered by a tall anticyclone accompanied by warm air ((3)).

- Typhoons Talim, Doksuri and Khanun moved northward near the Philippines, and cumulus convective activity around these masses was significantly higher than normal ((4)). This was a factor behind the strengthened extension of the Pacific High and the northward shift of the STJ (known as the Pacific – Japan (PJ) pattern⁵).
 - The conditions near the Philippines may be related to a number of factors, including an area of active cumulus convection (including typhoons) moving northwest over the tropical western Pacific ((4)) and upper-level cold vortices separating from a deeper-than-normal pressure trough over the northeastern North Pacific ((5)). Other potential factors include higher-than-normal sea surface temperatures (SSTs) in the tropical western North Pacific and suppressed convection in the tropical Indian Ocean ((6)), where the SST remained lower relative to other tropical oceans until summer. Both of the latter are likely related to the La Niña event that ended in winter 2022/23.
- Quasi-stationary Rossby wave propagation from Europe and the Mediterranean Sea (known as the Silk Road teleconnection) may also have contributed to the northward shift of the STJ near Japan from late July to mid-August onward ((2), (3)).
- In addition to the strengthening of the Pacific High and the northward shift of the STJ, a rise in global temperatures is thought to have further contributed to the remarkably high temperatures.
 - Event attribution science, in which the effects of global warming are evaluated ((7)), suggests that the probability of high temperature events is now higher than in a situation with no global warming.
- In early August, Typhoon Khanun remained near Okinawa/Amami before slowly moving northward over the sea to the west of Kyushu. Typhoon Lan then slowly moved northward from the south of Japan to the Sea of Japan in early/mid-August. As a result, warm and moist air flowed from the south around these typhoons in the vicinity of Japan. Additionally, as the Pacific High's extension toward Japan weakened slightly, flow from the High's margins contributed to a remarkable rise in temperature, especially on the Sea of Japan side, due to Foehn phenomena.
- The northerly shift of the STJ continued to be evident near Japan, and its coverage with warmer-than-normal air is thought to have contributed to the remarkably high temperatures.

(b) Effects of record-high SST around northern Japan

The SST around northern Japan reached a record high (Figure 2-6), especially off the Sanriku coast where the Kuroshio Extension was displaced far northward, and temperatures

⁵ When cumulus convective activity near the Philippines is more active than normal, the low-pressure part of the lower atmosphere (monsoon trough) and associated counterclockwise circulation seen from Southeast Asia to the Philippines during the summer season are stronger than normal, and air rising near the Philippines descends near Japan, strengthening the Pacific High's extension over the country's Honshu mainland.

remained remarkably high from the surface to the interior of the ocean ((8)). The high SST hindered lower-atmosphere cooling in the northern part of the Sea of Japan and from southeast Hokkaido to the area off Tohoku, which may have contributed to the record-high temperature in northern Japan. The high SST may also have prevented the formation of marine low-level cloud, which contributed to high temperatures in coastal areas and a further SST rise due to increased solar radiation (Figure 2-7).

(3) Climate characteristics and factors behind remarkably high temperatures worldwide

The World Meteorological Organization (WMO) also reported abnormally high temperatures and other extreme events in many parts of the world in July 2023 (see WMO News on 14 August⁶ and Figure 2-8 from TCC/JMA analysis). Daily maximum temperatures exceeded 45°C, which was significantly higher than normal, along the Mediterranean coast and in the southern part of the United States. The anomaly of the preliminary world average temperature (i.e., for land and sea surfaces) for July was +0.62°C higher than the standard 30-year average from 1991 to 2020 according to JMA analysis. This surpassed the values for 2016 and 2021 (+0.29°C), which were the previous highest since 1891 when records began. In addition, the monthly global average temperature was the highest for May, June, July and August 2023.

As shown in Figure 2-9 (with the numbers in parentheses here corresponding to the figure), these remarkably high temperatures were due to record highs overall in tropical regions in association with El Niño conditions ((1)). In the mid-latitudes of the Northern Hemisphere, regions where the upper STJ meandered northward ((2)) were covered by warm high-pressure systems, and were also influenced by overall high tropospheric temperatures due to global warming ((3)). These phenomena are thought to have resulted in remarkably high temperatures similar to those seen in Japan. In the high latitudes of the Northern Hemisphere, increased temperatures were observed due to a large meandering of the polar frontal jet stream ((4)).

⁶ <https://public.wmo.int/en/media/news/july-2023-confirmed-hottest-month-record>

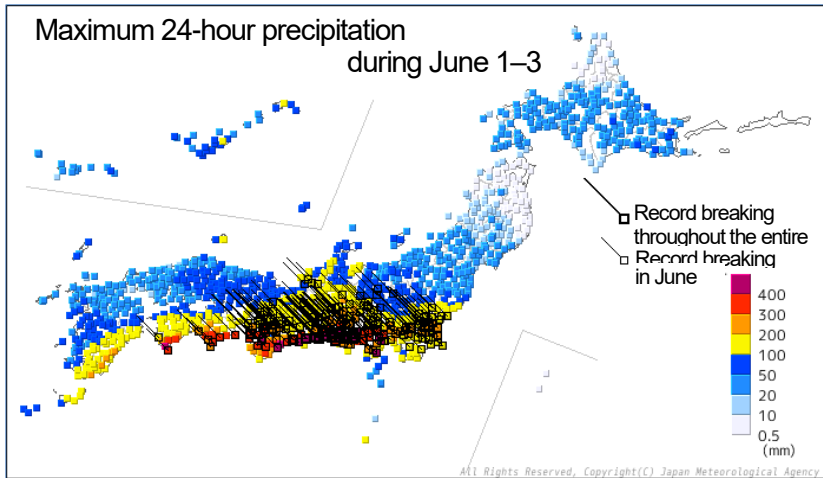


Figure 1-1. Maximum 24-hour precipitation during June 1 - 3

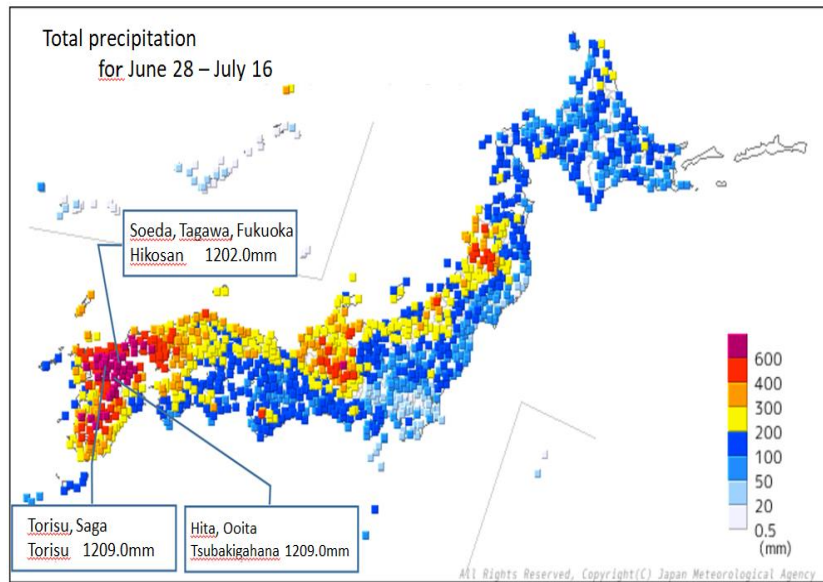


Figure 1-2. Total precipitation for June 28 - July 16

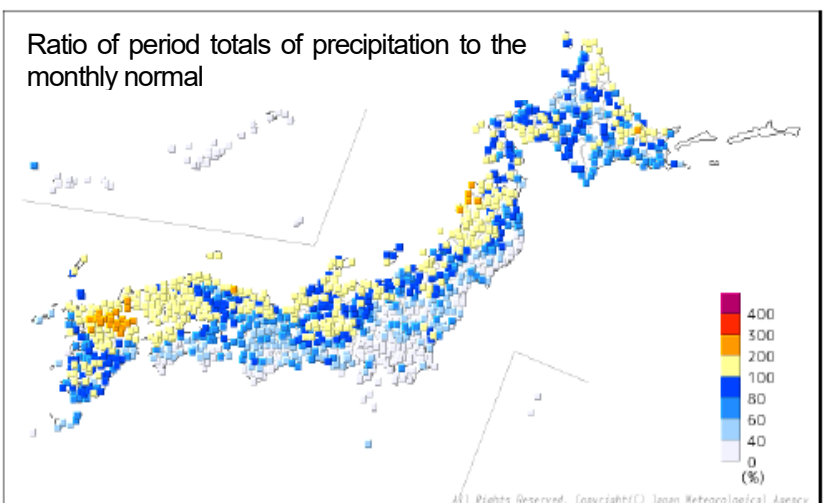


Figure 1-3. Ratio (%) of period totals of precipitation to the monthly normal of July

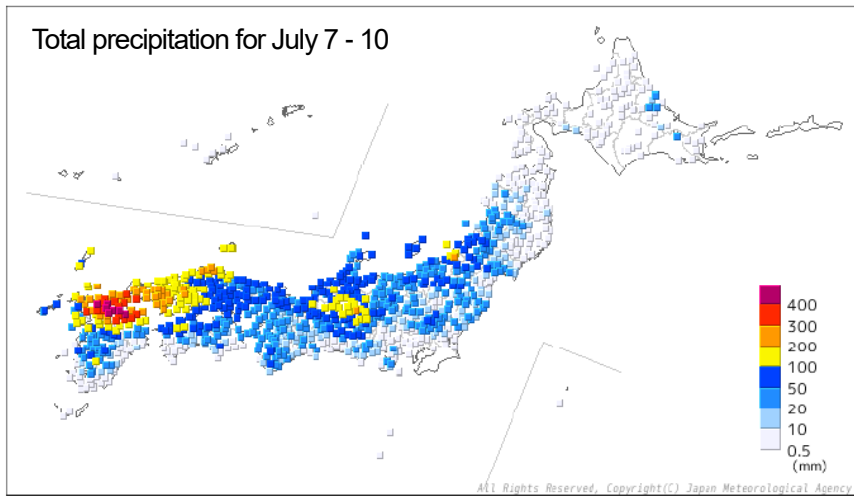


Figure 1-4. Total precipitation for July 7 - 10

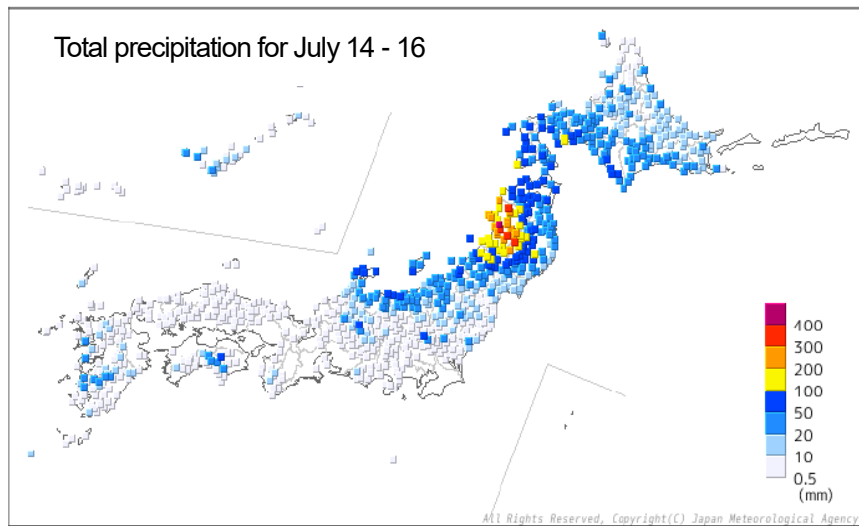


Figure 1-5. Total precipitation for July 14 - 16

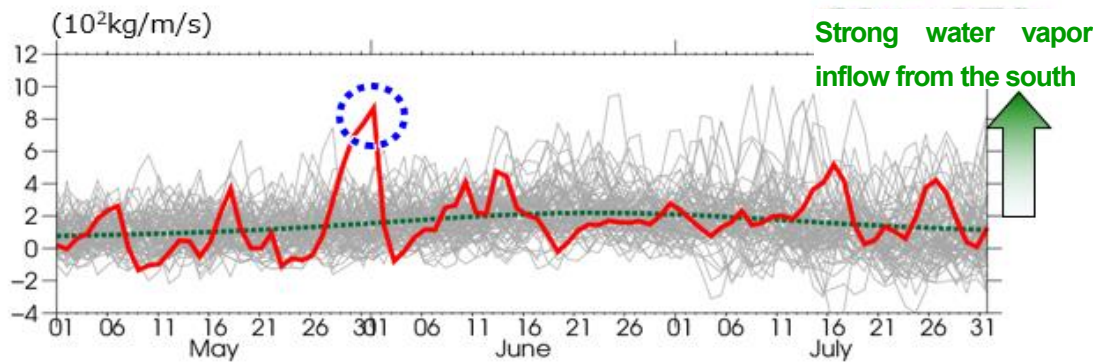


Figure 1-6. Daily time-series representation (May – July) of the intensity of northward moist air flow (vertically accumulated water vapor flux) in the troposphere averaged over the south of Japan (20 – 30°N, 125 – 135°E)

The red line is for 2023, the grey lines indicate individual years from 1948 to 2022, and the green line indicates the normal. The unit is 10^2 kg/m/s. The blue circle indicates the beginning of June 2023. Based on JRA-3Q.

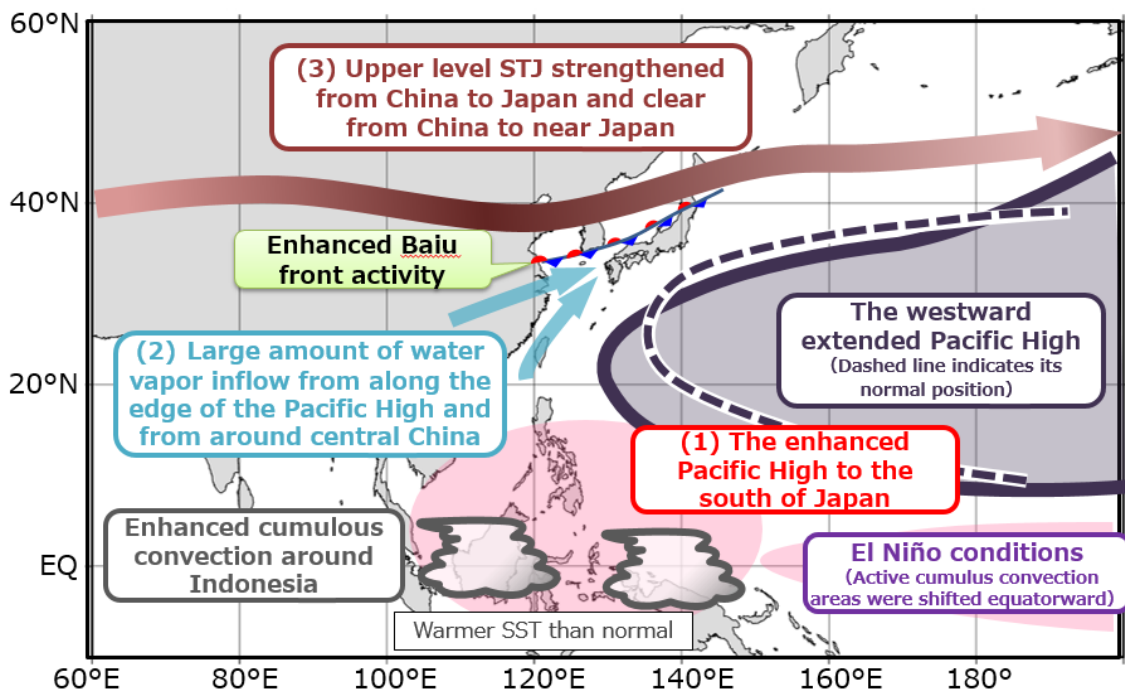
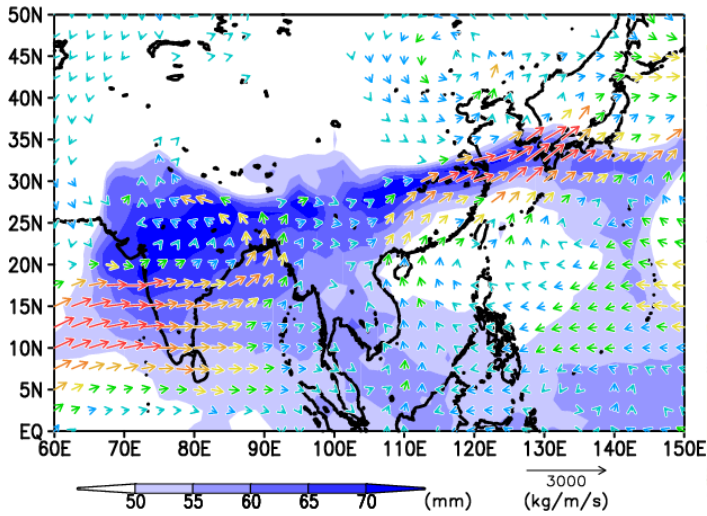


Figure 1-7. Characteristics of atmospheric circulation bringing heavy rainfall from late June to mid-July



July 10

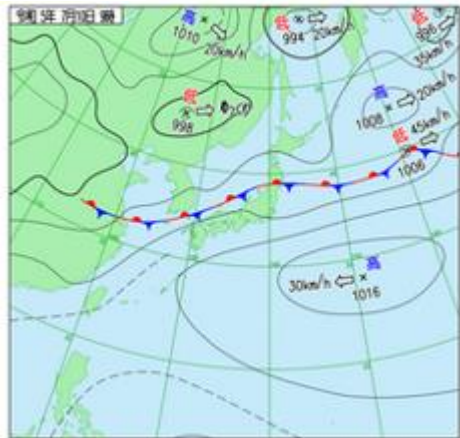
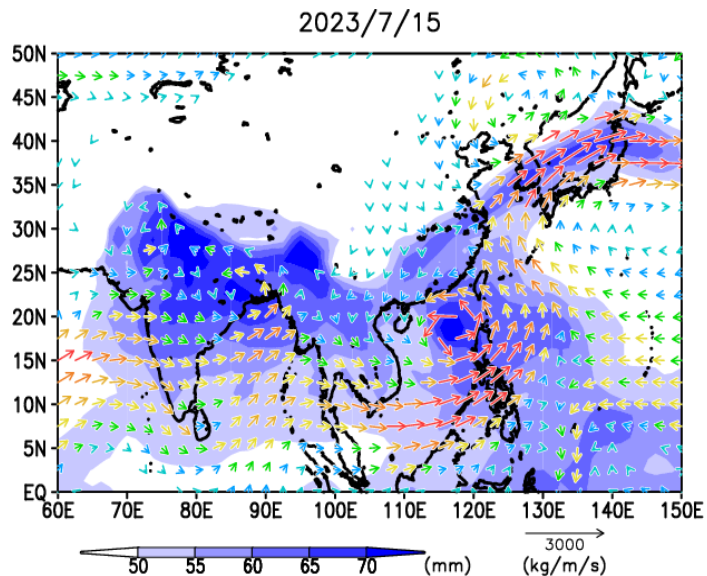


Figure 1-8. Left: flow of water vapor averaged for July 7 – 10; right: surface weather map for 09 JST, July 10

In the figure on the left, shading represents amounts of water vapor (precipitable water, mm), and arrows represent vertically integrated water vapor flux in kg/m/s. Arrows in warmer colors indicate stronger flow. Vertical accumulation is up to 300 hPa (altitude approx. 9,500 m) from the ground. Based on JRA-3Q.



July 15

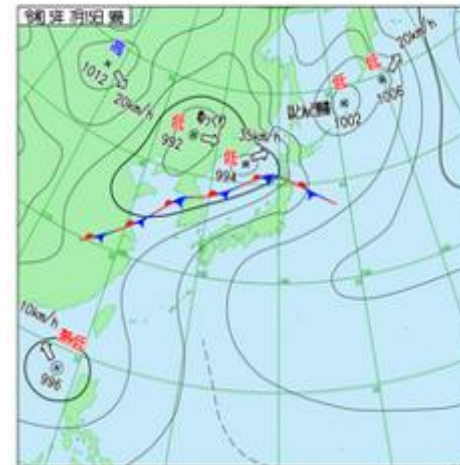


Figure 1-9. Left: flow of water vapor for July 15; right: surface weather map for 09 JST, July 15

In the figure on the left, shading represents amounts of water vapor (precipitable water, mm), and arrows represent vertically integrated water vapor flux in kg/m/s. Arrows in warmer colors indicate stronger flow. Vertical accumulation is up to 300 hPa (altitude approx. 9,500 m) from the ground. Based on JRA-3Q.

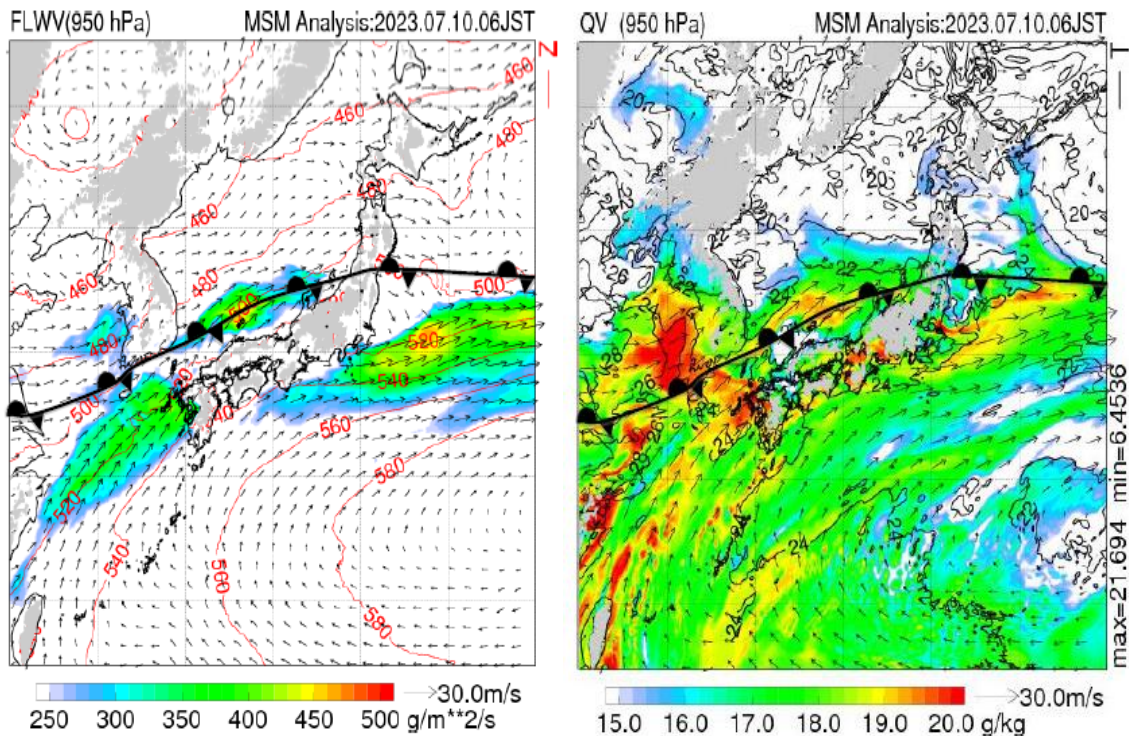


Figure 1-10. Left: water vapor inflow (g/m²/s); right: specific humidity (g/kg) at 950 hPa (altitude approx. 500 m) for 06:00 JST on July 10
 In the figure on the left, water vapor inflow (altitude (m)) is shown by red lines. In the figure on the right, specific humidity (temperature in °C) is shown by black lines. Wind (black arrows) and Baiu front positioning are also indicated. The data source is JMA's meso-objective analysis.

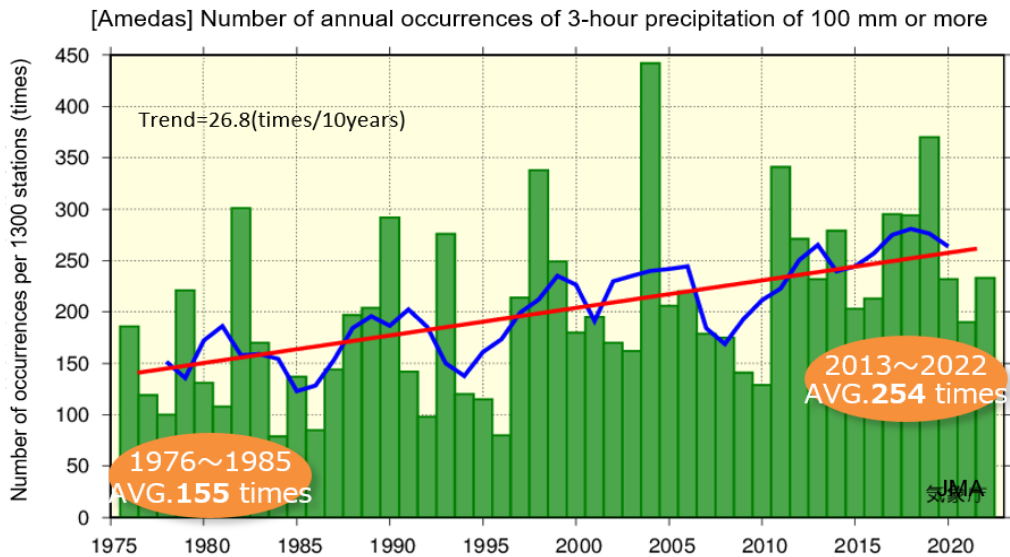


Figure 1-11. Annual number of rain events exceeding 100 mm/h (1976 – 2022)
 Green bars show the annual number of events for each year (converted from nationwide AMeDAS observations at 1,300 locations), the blue line shows the 5-year moving average, and the red line shows the long-term trend of change (averaged for the whole period).

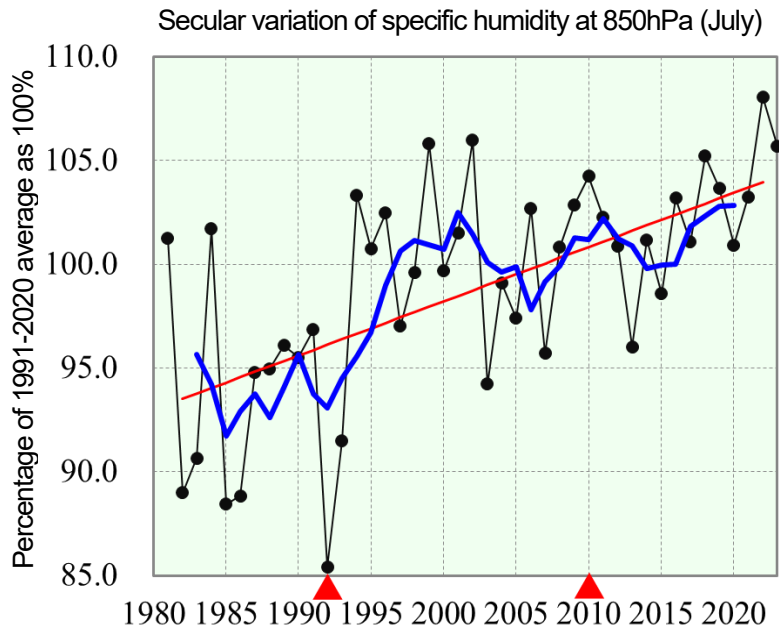


Figure 1-12. Secular change in the ratio of monthly mean specific humidity (water vapor content per kilogram of air) to the reference value at 1,500 m (850 hPa) in July over Japan (period: 1981 – 2023)

The black line shows the ratio (%) to the reference value at 13 high-altitude meteorological observation stations in Japan (Wakkanai, Sapporo, Akita, Wajima, Tateno, Hachijojima, Shionomisaki, Fukuoka, Kagoshima, Nase, Ishigakijima, Minamidaitojima and Chichijima). The blue line indicates the five-year moving average, and the red line indicates the long-term trend of change (statistically significant at the 99% confidence level). The reference is the average from 1991 to 2020; slightly higher relative values may be observed due to instrumentation changes (▲).

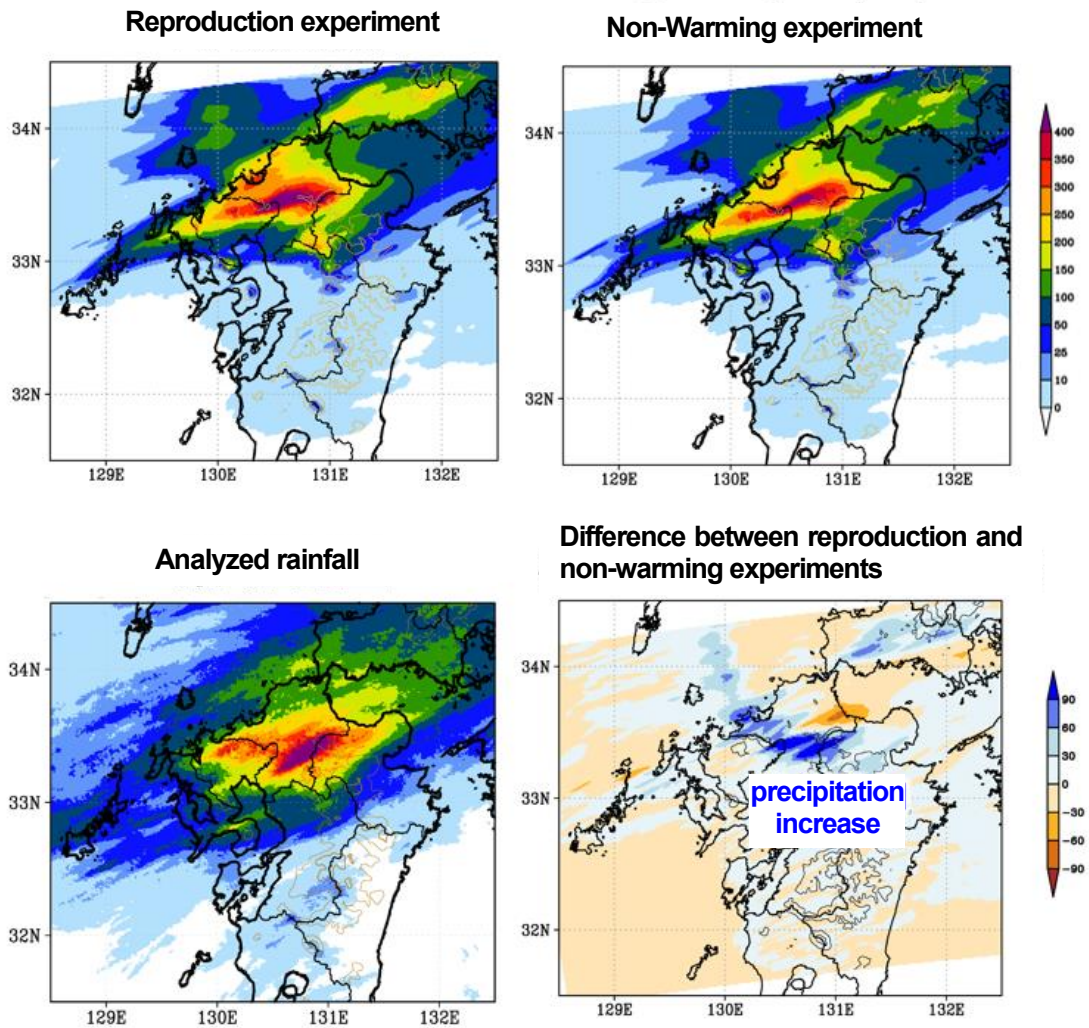


Figure 1-13. Results of quantitative event attribution experiments

Ensemble-averaged precipitation from an eight-member reproduction experiment (upper left) and a non-warming experiment (upper right), in which the warming difference was removed, using the JMA non-hydrostatic model (JMA-NHM) with initial values from three-hourly meso-objective analysis for July 7 – 8. The forecast covers 36-hour integrated precipitation from 09 h on July 9 to 21 h on July 10. The bottom right figure shows the difference between the two, and the lower left figure shows analytical cumulative rainfall from 09 h on July 9 to 21 h on July 10.

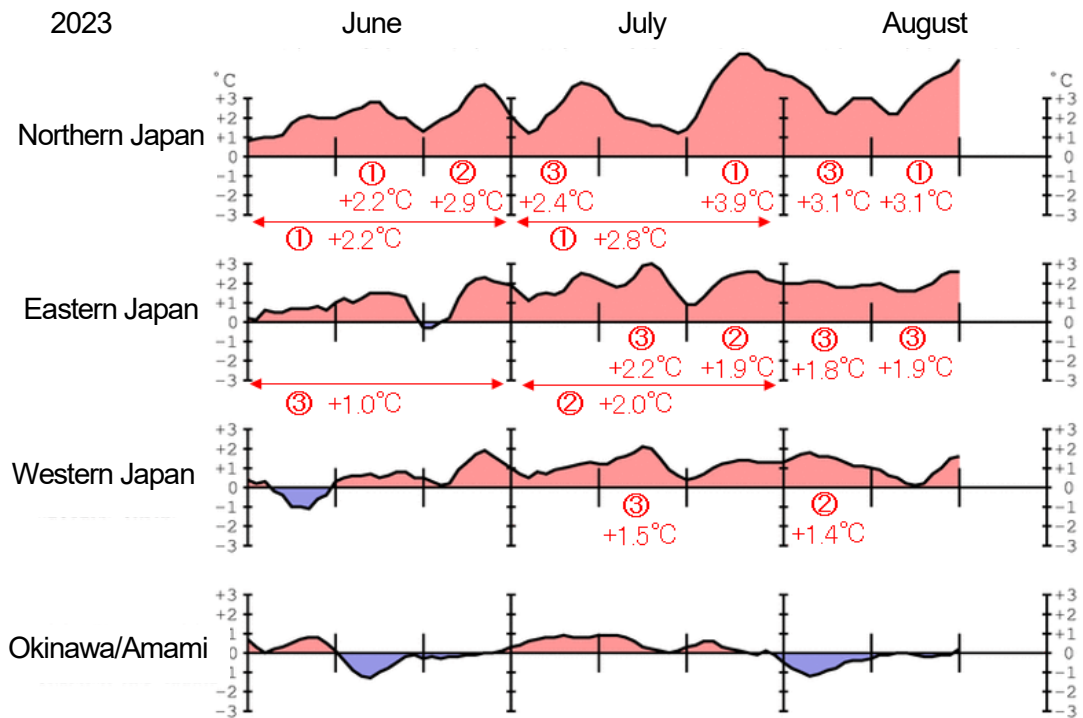


Figure 2-1. Time-series representations of five-day running mean temperature anomalies (°C) for June – August 2023

The base period for the normal is 1991 – 2020. The red circled numbers and values indicate the rank from highest average temperatures since 1946 and anomalies for each month and each ten-day period (up to the top three) as of August 24.

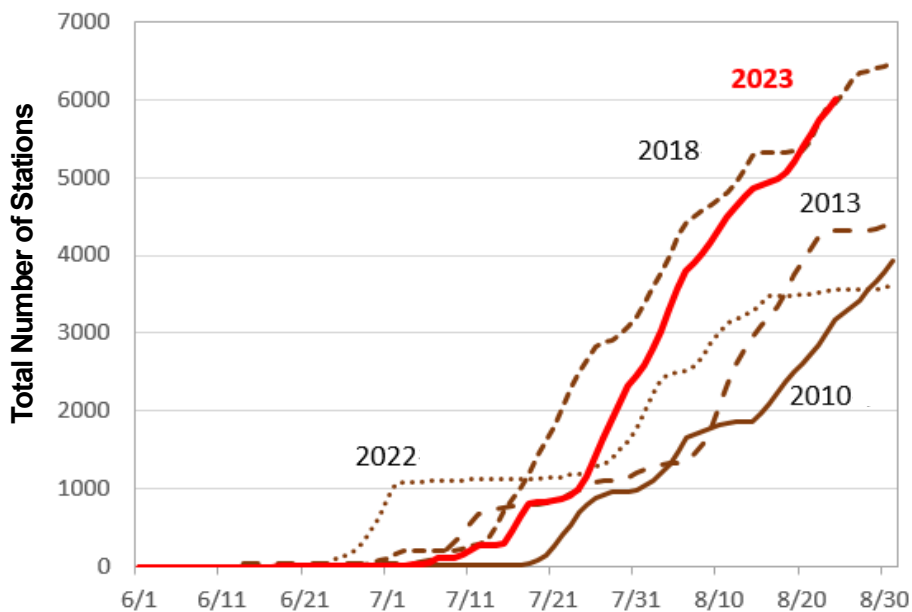


Figure 2-2. Cumulative numbers of extremely hot days (daily maximum temperatures above 35°C) observed at AMeDAS stations nationwide

Results for June 1 – August 31 (red line: 2023 up to August 24) and previous hot years since 2010. The total numbers of AMeDAS stations as of June 1 were 919 for 2010, 927 for 2013 and 2018, 914 for 2022, and 915 for 2023.

Mean temperature anomalies in July in Japan

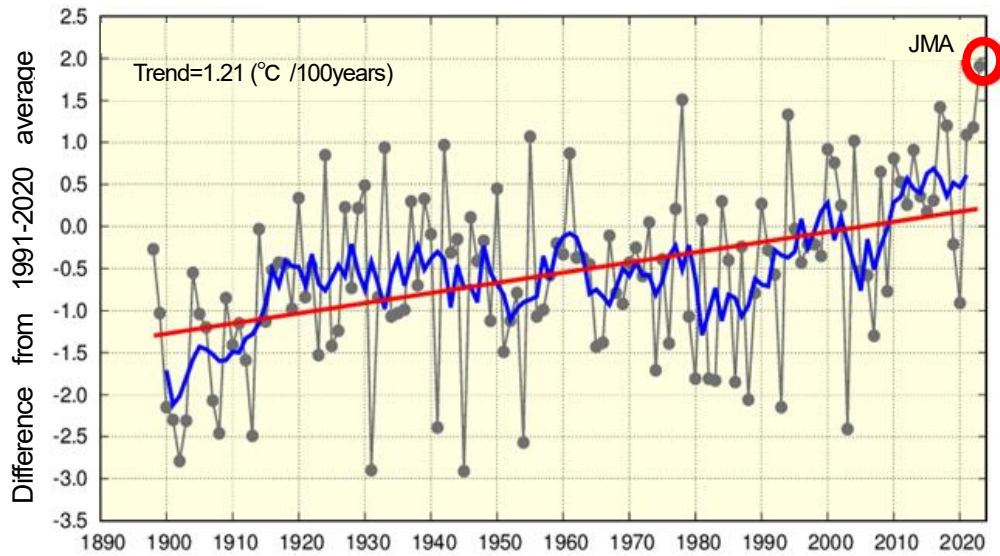


Figure 2-3. Average temperature deviation in Japan in July for 1898 – 2023

The base value for deviations is the normal for 1991 – 2020. The black line shows the average of deviations from this value for individual years at 15 observation stations in Japan, the blue line shows the five-year moving average of the deviations, and the red line shows the long-term trend of change (the average for the whole period). The red circle indicates July 2023.

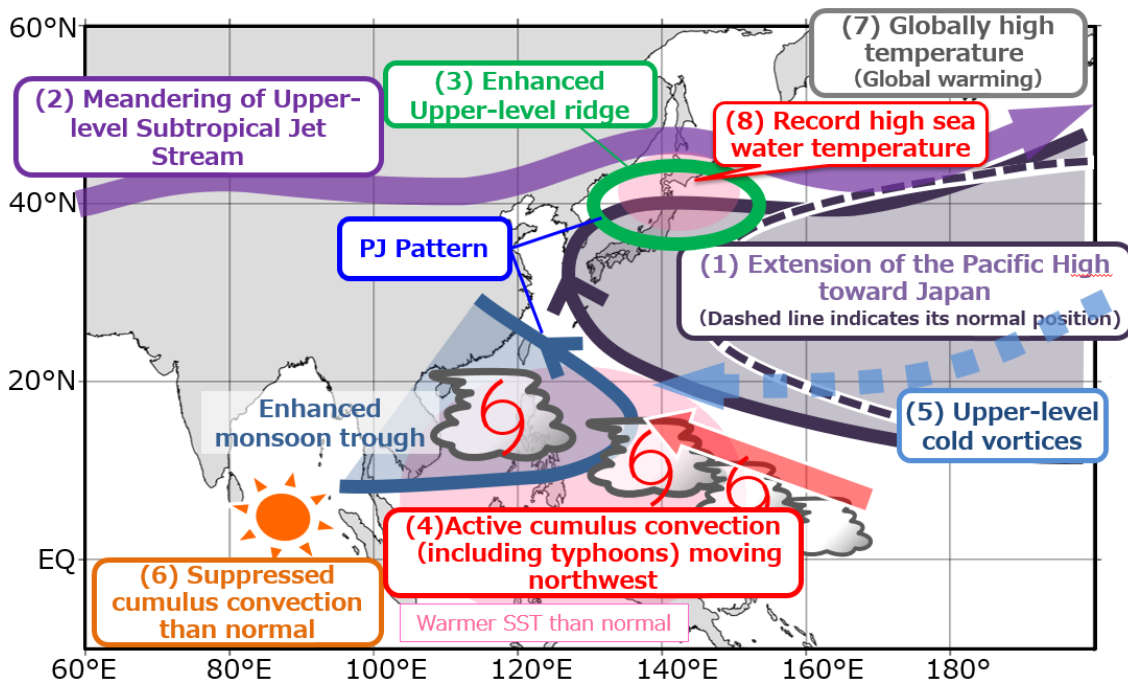


Figure 2-4. Characteristics of large-scale atmospheric circulation bringing extremely high temperatures

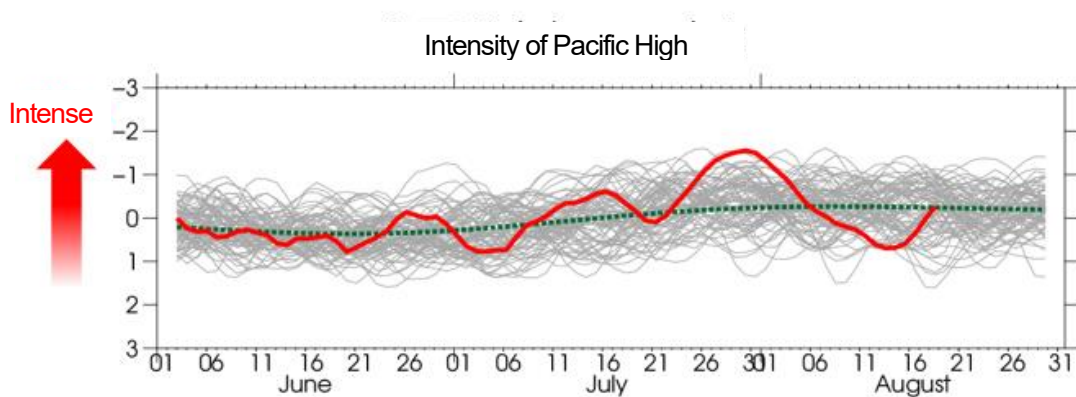


Figure 2-5. Changes in anticyclone intensity around Japan for individual years (June 1 – August 31)

Five-day moving averages of anticyclone intensity (relative vorticity, unit: $10^{-5}s^{-1}$, vertical axis inverted up and down) averaged over the area between $30^{\circ}N$ – $40^{\circ}N$ and $120^{\circ}E$ – $150^{\circ}E$ in the lower troposphere (approx.. 1,500 m height). The red line represents 2023 (based on data up to August 20), the green line represents the normal (1991 – 2020 average), and the grey line represents 1948 – 2022. Negative and larger values indicate stronger anticyclones. Based on JRA-3Q.

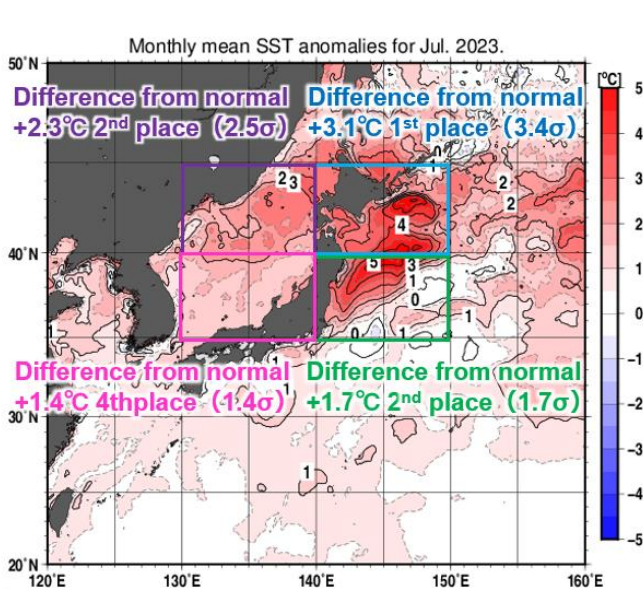


Figure 2-6. Distribution of July mean sea surface temperature anomalies around Japan
The unit is $^{\circ}C$. Rankings are for July since 1982. σ indicates the interannual standard deviation.

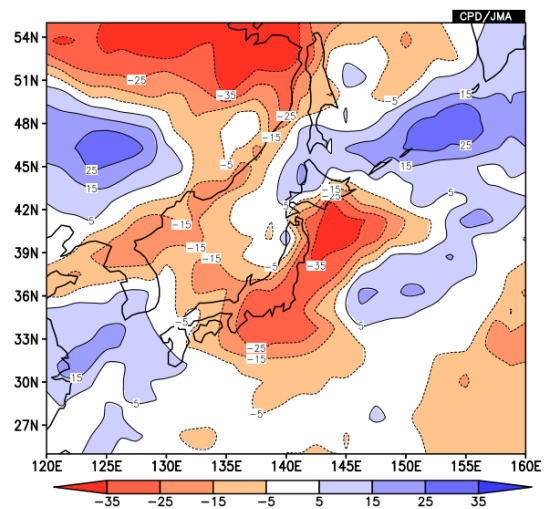


Figure 2-7 Deviation from the normal of upward shortwave radiation fluxes at the ground surface in July
Difference in upward shortwave radiation flux over the ground in July. Negative values with warmer colors indicate more solar radiation. The unit is W/m^2 . Based on JRA-3Q.

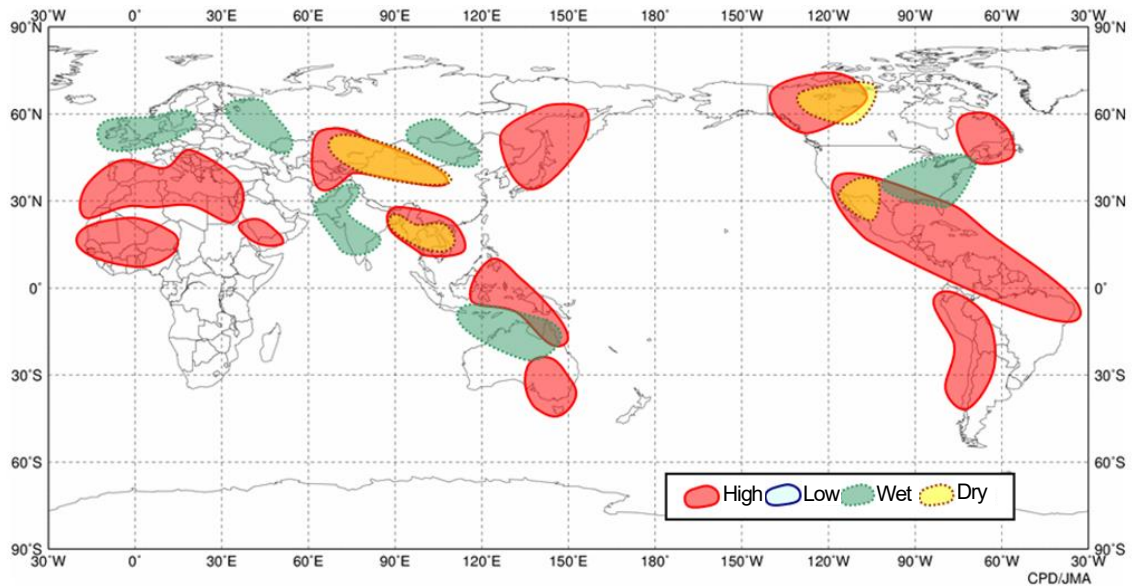


Figure 2-8. Extreme weather in the whole globe for July 2023

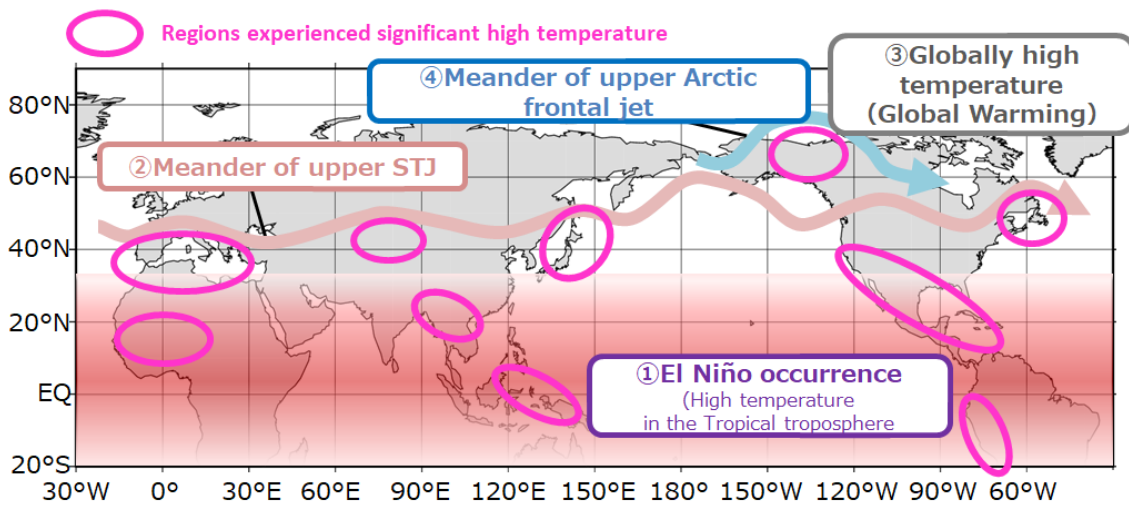


Figure 2-9. Characteristics of large-scale atmospheric circulation bringing significant high temperatures globally

The mid- and high-latitude regions where significantly high temperatures were observed are consistent with areas where the STJ and the frigid frontal jet stream continued to meander northward (e.g., along the Mediterranean coast).

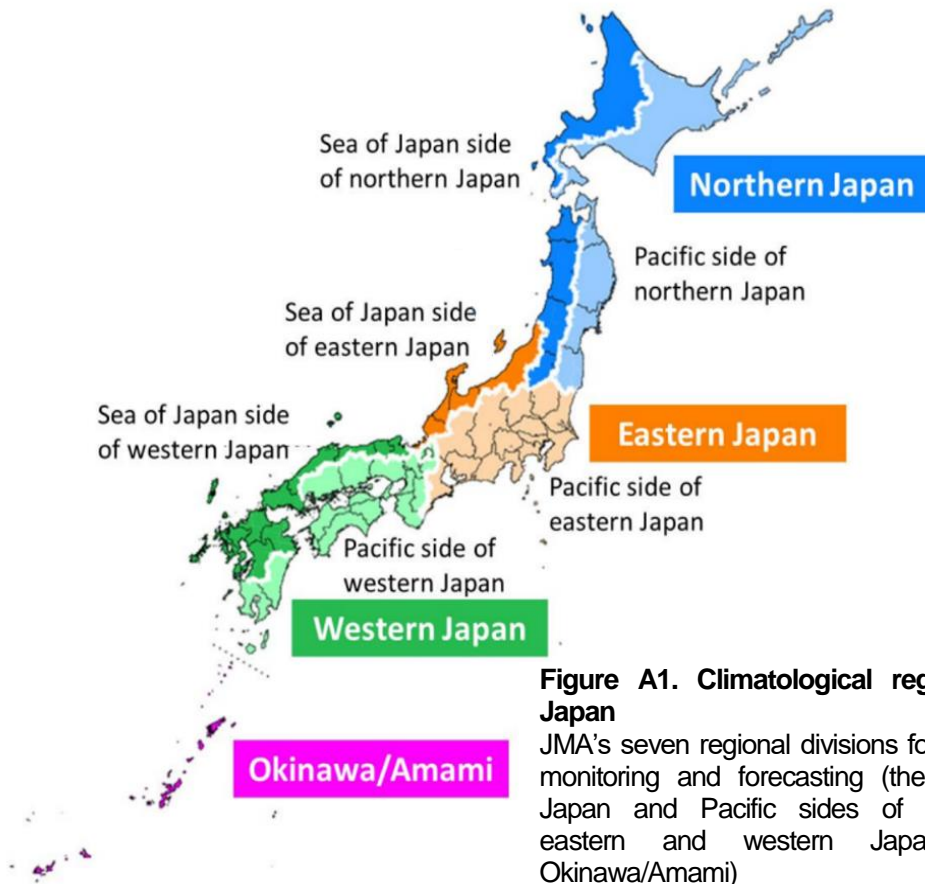


Figure A1. Climatological regions of Japan
 JMA's seven regional divisions for climate monitoring and forecasting (the Sea of Japan and Pacific sides of northern, eastern and western Japan, and Okinawa/Amami)